Sensors and Materials, Vol. 17, No. 4 (2005) 187–197
MYU Tokyo

S & M 0597

Arrhenius and Non-Arrhenius Behaviour During Anisotropic Etching

Miguel A. Gosálvez[1*], Risto M. Nieminen and Kazuo Sato[1]

Laboratory of Physics, Helsinki University of Technology, 02015 Espoo, Finland
[1]Dept. of Micro-NanoSystem Engineering, Nagoya University, Nagoya 464-8603, Japan

(Received October 1, 2004; accepted March 17, 2005)

Key words: Arrhenius and non-Arrhenius behaviour, anisotropic etching, apparent macroscopic activation energy, surface fractions, activity fractions

We present evidence from both simplified and realistic models of anisotropic wet chemical etching that the macroscopic etch rate can deviate from the linear Arrhenius temperature dependence. The results are rationalized by using the recently established formulation of the apparent macroscopic activation energy as an average over the microscopic activation energies, including a correction term. The study shows that care should be taken and crosschecking should be practiced when assigning the macroscopic activation energy to one (or more) atomistic process(es). In particular, we show that the fractions of removed particles should be used to decide the nature of the dominating process, not the surface fractions. We conclude that non-Arrhenius behaviour can be expected when the fractions of removed particles change significantly over the considered range of temperatures.

1. Introduction

During wet chemical etching of crystalline silicon the liquid-solid interface (surface) is an example of an evolving nonequilibrium open system driven by the environment through the removal of particles according to site specific reaction rates p_α. The fact that the experimental etch rate usually follows a linear Arrhenius dependence with temperature (displaying a constant apparent macroscopic activation energy $E_\alpha^{(1,2)}$) temptatively suggests that only one surface site type (from all the possible types $\alpha = 1, 2, ..., M$) dominates the macroscopic evolution of the surface and that the macroscopic activation energy simply corresponds to the microscopic activation energy E_α of that site (i.e., $E_a \approx E_\alpha$ for one specific site type α). Furthermore, since it should be possible to describe the apparent activation energy as a weighted average of the microscopic activation energies (i.e., $E_a \sim \sum_{\alpha=1}^{M} w_\alpha E_\alpha$), the constant-slope experimental behaviour suggests that one single

*Corresponding author, e-mail address: mag@kaz.mech.nagoya-u.ac.jp

site dominates the weighted average. A blind identification of the weights w_α as the surface fractions f_α eventually leads to the idea that the macroscopic activation energy corresponds to the activation energy of the majority sites on the surface. It is well known, however, that the etching process at Si(111) miscut surfaces proceeds by means of step propagation (which corresponds to the removal of minority sites) rather than by terrace-site removals (removal of majority sites). Thus, we are confronted with the following question: is etching really controlled by the majority sites as suggested by the linear Arrhenius behaviour or is it dominated by some minority sites, perhaps even several minority sites working together? How can we quantitatively determine which site is mostly responsible for the overall etching process?

In this article, we show that the direct assignment of the apparent activation energy to the majority sites should be avoided (even in the case of fully linear Arrhenius behaviour) and that the correct assignment to one or several surface sites requires the use of, not the relative appearance f_α of the different site types on the surface (surface fractions), but the relative removal $w_\alpha = f_\alpha p_\alpha / \sum_{\beta=1}^{M} f_\beta p_\beta$ of each site type as compared with all the other types (activity fractions). In other words, we show that it is the maximum activity fraction w_α that should be used to decide which is the dominating site, not the maximum surface fraction f_α.

We first motivate the necessity of understanding the relationship between macroscopic and microscopic activation energies, and present examples of both Arrhenius and non-Arrhenius behaviour that can be obtained from simplified and realistic models of anisotropic etching (Sections 2 and 3). This should underline the fact that the macroscopic activation energy does not necessarily correspond to only one surface site but it is rather some sort of nontrivial average of the microscopic activation energies. In Section 4, we present the correct relationship between the macroscopic and microscopic activation energies[3] and proceed to rationalize the obtained results. Finally, we draw our conclusions in Section 5.

2. Realistic Model for Anisotropic Wet Chemical Etching

Anisotropic wet chemical etching is a nonequilibrium process in which both the microscopic surface roughness and morphology, and the macroscopic orientation-dependent etch rate are essentially determined by the relative values of the microscopic (atomistic) reaction rates. The origin of the (large) differences in site-specific rates is found in two microscopic mechanisms:[4] the weakening of backbonds following OH termination of surface atoms and the existence of significant interaction between the terminating species (H / OH). As a result, the total (local) energy of a surface atom can be expressed as the sum of three terms:[5]

$$E = E_{\text{bonds}} + \sum \left(e_{\text{OH/H}}^{\text{TA}} + e_{\text{OH/OH}}^{\text{TA}} \right) + \sum \left(e_{\text{OH/H}}^{\text{FN}} + e_{\text{OH/OH}}^{\text{FN}} \right), \tag{1}$$

where E_{bonds} is the bonding energy that takes into account the bonds that exist with the first nearest neighbours and $\sum \left(e_{\text{OH/H}}^{\text{TA}} + e_{\text{OH/OH}}^{\text{TA}} \right)$ $\left(\sum \left(e_{\text{OH/H}}^{\text{FN}} + e_{\text{OH/OH}}^{\text{FN}} \right) \right)$ symbolically denotes the

total energy from the interactions between the OH groups terminating the target atom TA (the first neighbours FN) and H and/or OH terminating the indirect second neighbours of the target atom TA (first neighbours FN). The geometrical restrictions to hydroxyl termination in the presence of indirect second neighbours is a manifestation of the important role of steric hindrance in anisotropic wet chemical etching. In this model, the source of steric hindrance is identified as the (H/OH-terminated) indirect second neighbours.

The local dynamics of this model consists of random removals of surface sites with probabilities $p = p_0 e^{-\Delta E / k_B T}$, where ΔE is defined as the activation energy. Here, p_0 and E_c are parameters describing the different surface atom types (i.e., surface sites). The function max $(0, E - E_c)$ is used for implementing the Metropolis algorithm.[6] Following the discussion of Gosálvez *et al*. in,[5] and the notation used in surface studies of Si(111),[7] we consider the following surface site types:

1. Type 0: Nonbonded atoms that have not been removed: unlinked (UL)
2. Type 1: Singly bonded atoms: trihydrides (TRI); also referred to as kinks.
3. Type 2A: Doubly bonded atoms on ideal (100) surfaces: terrace dihydrides (TD)
4. Type 2B: Vertical doubly bonded atoms at ideal $\left[\bar{1}2\bar{1}\right]$ steps: vertical step dihydrides (VSD)
5. Type 2C: Horizontal doubly bonded atoms at ideal $\left[\bar{1}2\bar{1}\right]$ steps: horizontal step dihydrides (HSD); plus all other possible doubly bonded atoms.
6. Type 3A: Triply bonded atoms at ideal (111) surfaces: terrace monohydrides (TM)
7. Type 3B: Triply bonded atoms at ideal $\left[1\bar{2}1\right]$steps: step monohydrides (SM); plus all other possible triply bonded atoms.

The atoms of type 0 are included for completeness since they can occasionally appear in connection to the formation of overhangs. This is, however, a rare event in the simulations and has a negligibly small effect on the evolution of the surface. These atoms are removed (with probability one) as soon as they are encountered. Accordingly, one can say that in this model the surface contains M=6(+1) atom types.

Note that due to the different possible combinations of the terminating species H and OH around a surface site, the energy E and the activation energy ΔE take different values for atoms of the same type. The six pairs of parameters $(p_{0\alpha}, E_{c\alpha})$ for Types 1, 2A,... 3B can be determined by comparison with experimental results. One can choose the parameters so that the relative values of the etch rates of a number of surface orientations agree with those from an experiment. By adjusting the parameters $p_{0\alpha}$, the simulated etch rates can be shifted up/down in an Arrhenius plot. Similarly, the slopes of the etch rates can be controlled by tuning the parameters $E_{c\alpha}$. Alternatively, it is also possible to choose the parameters $(p_{0\alpha}, E_{c\alpha})$ on the basis of a comparison of the simulated surface morphology with that from experiments. An example of this approach is provided in ref. 8.

In this work, we consider the same two sets of values for the $(p_{0\alpha}, E_{c\alpha})$ parameters (Table 1) as for cases A and B in ref. 8. Although the gross morphologies of most surface orientations are similar for both parameter sets, case A leads to the formation of pyramidal hillocks on (100) and case B to the formation of round pits. Examples of the typical dependence of the etch rate on temperature and some morphologies obtained with this etching model can be seen in Figs. 1(a)–1(c) for case A.

Table 1

Summary of parameters for cases A and B. $p_{0\alpha} = e^{S_\alpha / k_B}$, $\alpha = 1, 2A, ...3B$. S_α measured in eV/K and $E_{c\alpha}$ in eV.

	S_1	S_{2A}	S_{2B}	S_{2C}	S_{3A}	S_{3B}
A	1.30×10^{-3}	1.10×10^{-3}	1.07×10^{-3}	1.10×10^{-3}	5.47×10^{-5}	2.59×10^{-4}
B	1.50×10^{-3}	1.75×10^{-3}	7.99×10^{-4}	1.75×10^{-3}	4.07×10^{-4}	1.03×10^{-3}

	E_1	E_{2A}	E_{2B}	E_{2C}	E_{3A}	E_{3B}
A	0.658	3.633	3.688	3.563	6.309	5.686
B	0.908	3.555	3.555	3.555	6.307	5.521

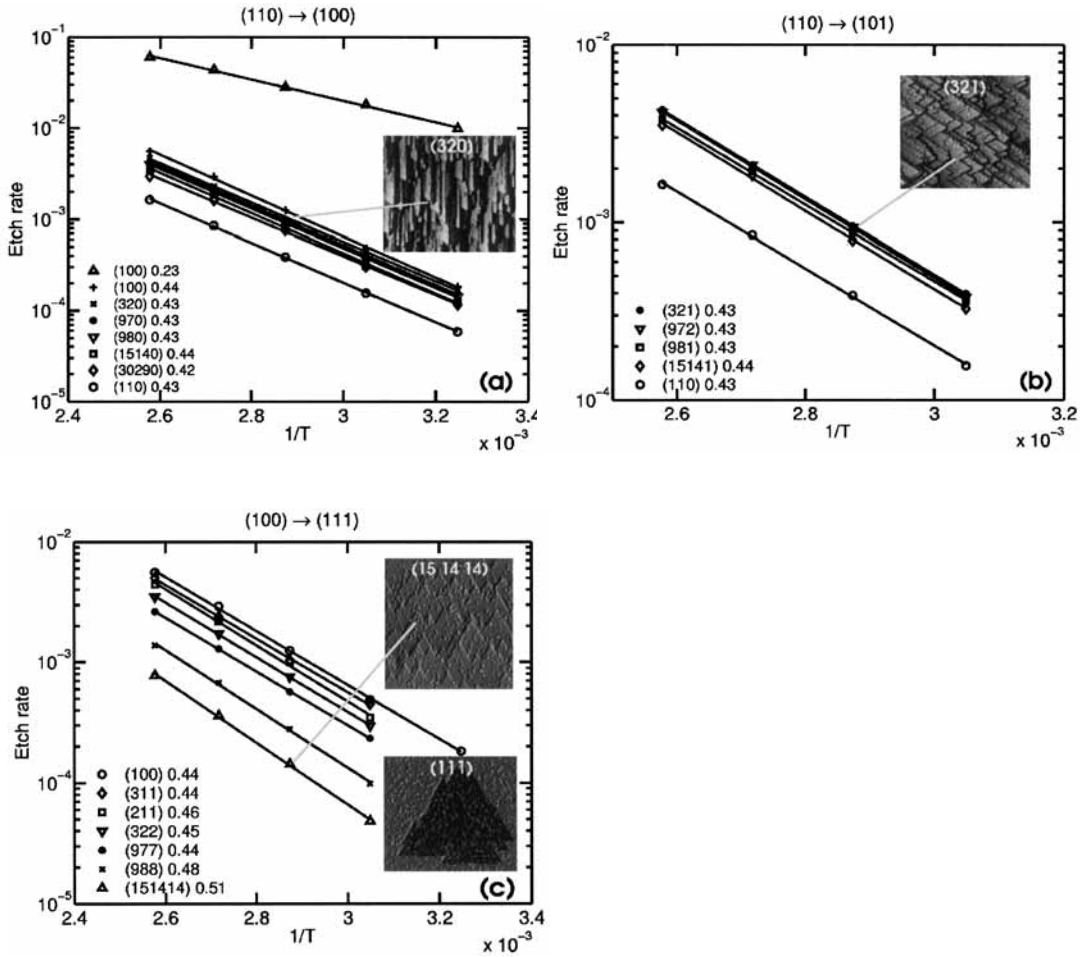

Fig. 1. Arrhenius behaviour of the etch rate for a number of crystallographic orientations using the parameter values of case A. A representative snapshot of the surface morphology for each series is shown in the inserts.

3. Thermal Flipping Chessboard (TFC)

The thermal flipping chessboard (TFC) is an analytically solvable, simplified model for anisotropic wet chemical etching.[3] The model considers a (two-dimensional) system with N total sites that can belong to M possible site types $\alpha = 1, 2, ..., M$ and can be removed from the system with probabilities $p_\alpha = p_{0\alpha} e^{-\Delta E_\alpha / k_B T}$ independently of the state of the neighbouring sites. The removal of a site of type α leads to the appearance of a site of type $\beta = 1, 2, ..., M$ with probability $\pi_{\alpha\to\beta}$. Thus, the transition matrix $\prod = (\pi_{\alpha\beta}) \equiv (\pi_{\alpha\to\beta})$ characterizes the probability of any conversion between the M species.

The TFC model contains the fundamental components for the simulation of chemical etching, namely, that the removal of one surface site produces the incorporation of new sites into the surface. However, it disregards the changes that might occur in the site types of the neighbouring surface sites. Although this somewhat limits the predicting power of the model for realistic applications, most features of the etching process can be easily studied with this simplified approach.

The important feature of the TFC model is that the transition matrix ($\pi_{\alpha\beta}$) is an external parameter, independent of other variables such as the removal probabilities p_α and the temperature T. The independence of Π from temperature allows the TFC model to be solved analytically exactly for any number M of particle types. The possibility of comparison to exact values makes the TFC systems ideal for testing and judging new ideas and/or strategies for the simulation of anisotropic etching.

Figure 2(a) shows a typical Arrhenius plot for the total removal rate versus inverse temperature for the TFC model with three types of particle ($M = 3$). Here, we have used the values described in ref. 3 for the parameters $p_{0\alpha}$, ΔE_α, and Π:

$$\begin{pmatrix} p_{01} \\ p_{02} \\ p_{03} \end{pmatrix} = \begin{pmatrix} 1.0 \\ 5\times10^{3} \\ 2\times10^{6} \end{pmatrix}; \begin{pmatrix} \Delta E_1 \\ \Delta E_2 \\ \Delta E_3 \end{pmatrix} = \begin{pmatrix} 0.0 \\ 0.3 \\ 0.5 \end{pmatrix}; \prod = \begin{pmatrix} 0.00110 & 0.08056 & 0.91834 \\ 0.02937 & 0.47202 & 0.49861 \\ 0.03961 & 0.58581 & 0.37458 \end{pmatrix} \tag{2}$$

Note that the exact solution does not follow linear behaviour exactly, as implied by the non-constant value of the activation energy E_a (i.e., the slope) in the insert. As Figs. 2(b)–2(d) show, this behaviour manifests itself in the form of strongly non-linear curves for the surface fractions, particularly in the case of the majority species (Figs. 2(c)–2(d)). These plots illustrate the fact that the combination of microscopic removal rates that follow the Arrhenius behaviour does not guarantee linear Arrhenius behaviour for the global macroscopic rate. The question is whether this non-Arrhenius behaviour is an artifact due to the simplifications made in this model or whether it can also be obtained in more realistic approaches, particularly in view of the fact that the realistic model of Section 2 produces linear Arrhenius behaviour for all surface orientations.

In order to address this point, we have conducted simulations for the same orientations as those shown in Fig. 1 using the realistic model with the parameter values of case B. The results are shown in Figs. 3(a)–3(c). The existance of non-Arrhenius behaviour is

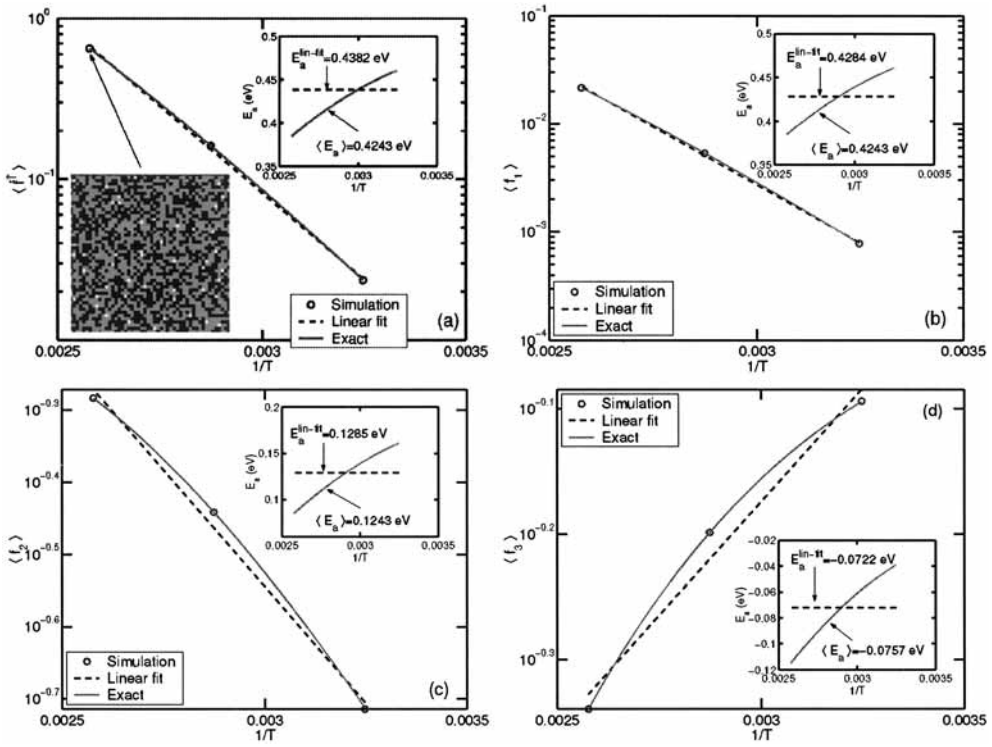

Fig. 2. A typical Arrhenius plot of (a) the total rate of removal of particles and the (average) surface fractions (b) $\langle f_1 \rangle$, (c) $\langle f_2 \rangle$, and (d) $\langle f_3 \rangle$ for the TFC model with $M = 3$. A representative snapshot of the system is shown in the insert in (a).

particularly clear for the orientations in the (100)→(111) series of Fig. 3(c). This shows that the behaviour depends on the choice of parameters and is not an anomaly or an artifact associated with one particular model.

These examples show that, from a theoretical perspective, both Arrhenius and non-Arrhenius behaviour are possible, underlining the fact that the macroscopic activation energy does not necessarily correspond to only one surface site but is rather some kind of nontrivial average of the microscopic activation energies. The previous examples demostrate the need to understand the relationship between macroscopic and microscopic activation energies. Furthermore, we need to understand why the behaviour is Arrhenius in some cases and non-Arrhenius in other cases.

4. Relationship Between Macroscopic and Microscopic Activation Energies

The previous results suggest that the macroscopic activation energy is a nontrivial function of the microscopic activation energies. The specific mathematical form of this function has been established recently.[3] As it turns out, the apparent macroscopic

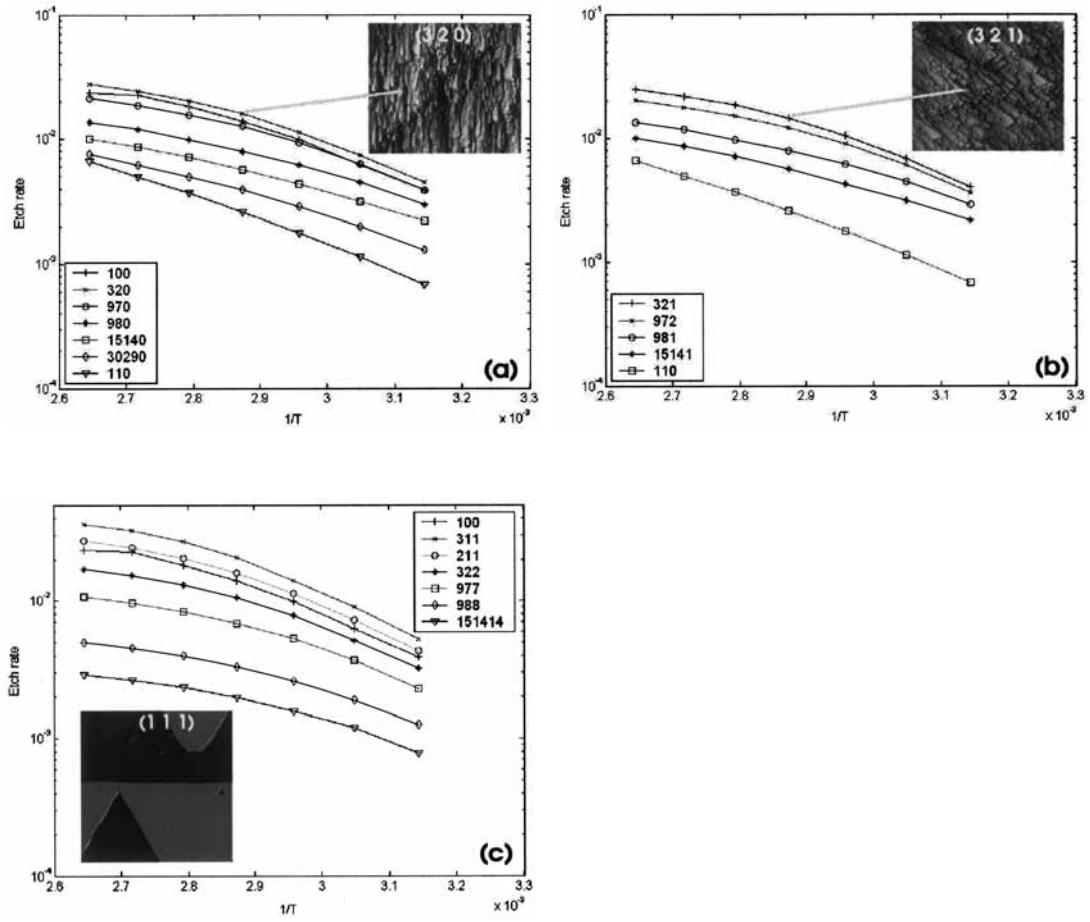

Fig. 3. Non-Arrhenius behaviour of the etch rate for a number of crystallographic orientations using the parameter values of case B. A representative snapshot of the surface morphology for each series is shown in the inserts.

activation energy E_a is only partially explained by the expected expression for the average of the microscopic activation energies $E_a^{(p)} = \sum_\alpha w_\alpha E_{p_\alpha}$ and a correction term accounting for the temperature dependence of the surface fractions $E_a^{(f)} = \sum_\alpha w_\alpha E_{f_\alpha}$ has to be included:

$$E_a = E_a^{(p)} + E_a^{(f)} = \sum_\alpha w_\alpha \left(E_{p_\alpha} + E_{f_\alpha} \right) \tag{3}$$

Here, the weights w_α are the activity fractions defined in Section 1, E_{p_α} is the microscopic activation energy of the α-type sites (i.e., the slope of p_α in an Arrhenius plot) and E_{f_α} is the corresponding slope of f_α in such a plot. Note that one can always define an effective activation energy $E_a^{\text{eff}} = E_{p_\alpha} + E_{f_\alpha}$ for each surface type so that the macroscopic activation energy can be formulated as a simple weighted average:

$$E_a = \sum_\alpha w_\alpha E_\alpha^{\text{eff}} . \tag{4}$$

As an example of the use of eq. (3), Fig. 4(a) shows the etch rates of (100) and (110) obtained using the parameter values of case A for the realistic model. In order to understand the origin of the macroscopic activation energy for the case of (100), the first term $E_a^{(p)}$ in eq. (3) is obtained as the weighted sum of the microscopic activation energies shown in Fig. 4(b) and the second term $E_a^{(f)}$ is obtained as the weighted sum of the microscopic activation energies shown in Fig. 4(c). Figure 5(a) shows that $E_a^{(p)}$ accounts for about 72% of E_a whilst $E_a^{(f)}$ accounts for the remainder. Similar results are obtained for the case of (110). Note that, in the case of non-Arrhenius macroscopic behaviour a similar study can be made for the temperature dependence of the surface fractions using fitting functions that deviate from the linear case.

The activity fractions w_α can be used as indicators of the relative contributions of the different surface sites to the macroscopic activation energy. Figure 5(b) shows that the weights w_α are good approximations of the relative contributions ε_α of each atom type to the total macroscopic activation energy, defined as:

$$\varepsilon_\alpha = \frac{w_\alpha E_\alpha^{\text{eff}}}{\sum_\beta w_\beta E_\beta^{\text{eff}}} . \tag{5}$$

This feature allows for the unambiguous identification of the particular surface sites that effectively control the etching process. As an example, Fig. 5(b) shows that under the conditions of case A the etching process at both (100) and (110) is dominated by the removal of horizontal step dihydrides (2C), which corresponds to a minority site appearing on less than 1% of the surface according to Fig. 4(c) for (100). The vertical step dihydrides (2B) and the step monohydrides (3B) are next in importance in the etching process (Fig. 5(b)). Note that although the 3B sites are a majority site (about 40% of the surface) the 2B sites are minority (present less than 1%), as shown by Fig. 4(c). Similar results are obtained for the case of (110).

This analysis unambiguously establishes that the etching process in (100) under the chosen conditions (leading to the formation of pyramidal hillocks and texturized surfaces at the steady state here considered) consists of the propagation of monohydride-terminated steps (a majority site together with the terrace monohydrides, see Fig. 4(c)) by means of an unzipping process in which the removal of the step monohydrides triggers a local burst of

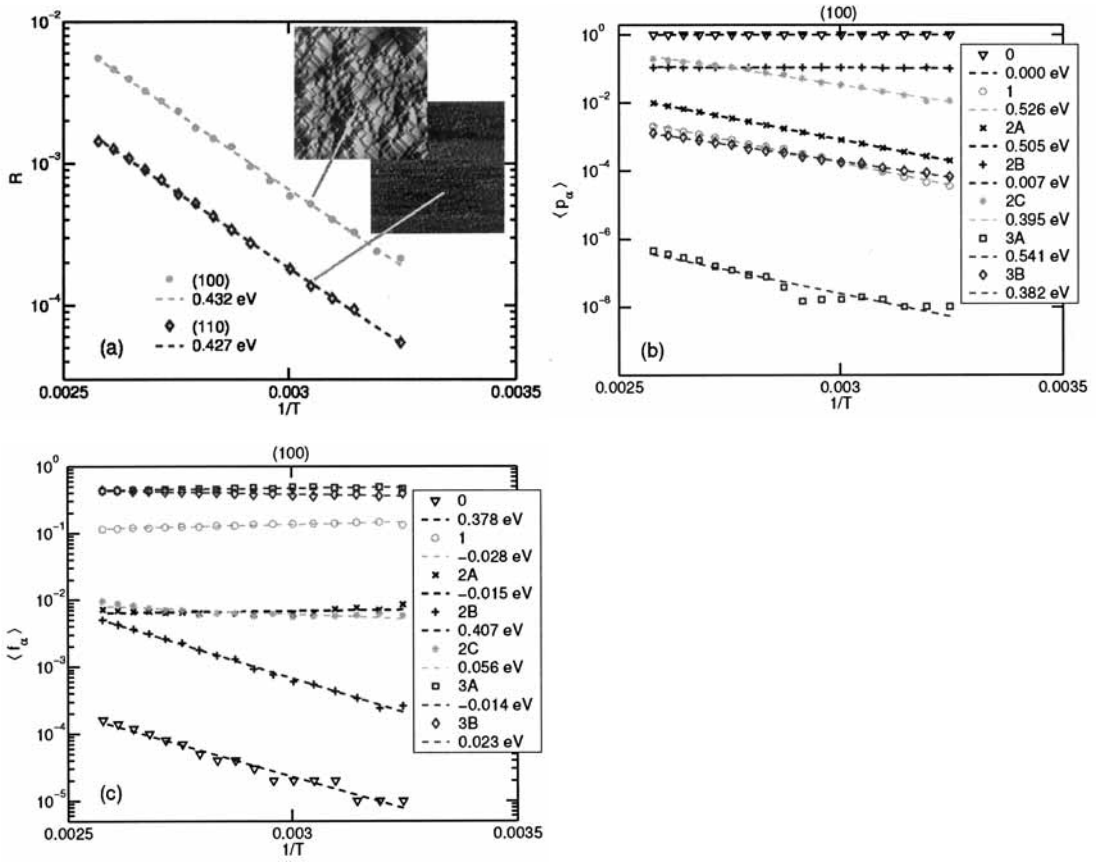

Fig. 4. Arrhenius plots for (a) the etch rates of (100) and (110); (b) the (average) removal rates $\langle p_\alpha \rangle$ for (100); and (c) the (average) surface fractions $\langle f_\alpha \rangle$ for (100). The parameter values of method A for the realistic model are used.

activity by enabling the removal of vertical and horizontal step dihydrides, as revealed by the high activity fractions for these two sites.

The previous analysis is an example of the use of the activity fractions in order to quantitatively measure the way in which the minority sites dominate the process. It also ilustrates the fact that the macroscopic activation energy is a complicated function and should not be identified with one atomistic process only; particularly not with the majority sites on the surface. We conclude that the activity fractions w_α should be used to decide the nature of the dominating species, not the surface fractions f_α.

Finally, let us note that, since the activity fractions are the relevant parameters for deciding on the relative role of the different surface sites, and, most importantly, since they can be used as good approximations of the relative contributions ε_α to the total macroscopic

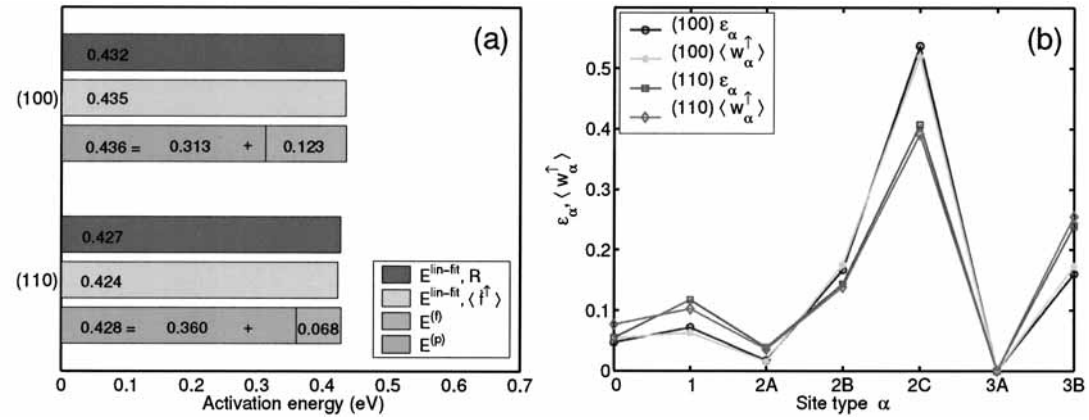

Fig. 5. (a) Macroscopic activation energies of (100) and (110) explained as the sum of two terms $E_a = E_a^{(p)} + E_a^{(f)}$. (b) Relative contributions of each surface site (α = 1, 2*A*, 2*B*,...) to the macroscopic activations energies of (100) and (110). Exact measured values (ε_α) and their approximations (w_α) are given.

activation energy, it becomes apparent that significant changes in the activity fractions within the explored range of temperatures will lead to the non-Arrhenius behaviour (see Fig. 6(a)). On the other hand, approximately constant activity fractions within the temperature range ensure a linear Arrhenius behaviour (see Fig. 6(b)). Note that, in this particular example, not only the activity fractions show larger slopes in Fig. 6(a) (as shown by the values of the quoted activation energies for sites 2C, 3B, 2B, and 1), but also two of the significant contributions (2B and 1) change so vigorously that they actually cross each other significantly. Note, however, that this crossing is not the origin of the non-Arrhenius behaviour. The only necessary condition for non-Arrhenius behaviour is a significant change in one or more of the dominant activity fractions.

5. Conclusions

By using simplified and realistic models of anisotropic wet chemical etching we show that the macroscopic etch rate can deviate from the linear Arrhenius temperature dependence. We conclude that the non-Arrhenius behaviour occurs when the activity fractions (i.e., the normalized fractions of removed particles) change significantly over the considered range of temperatures. In comparison, approximately constant activity fractions within the considered temperature range ensure linear Arrhenius behaviour.

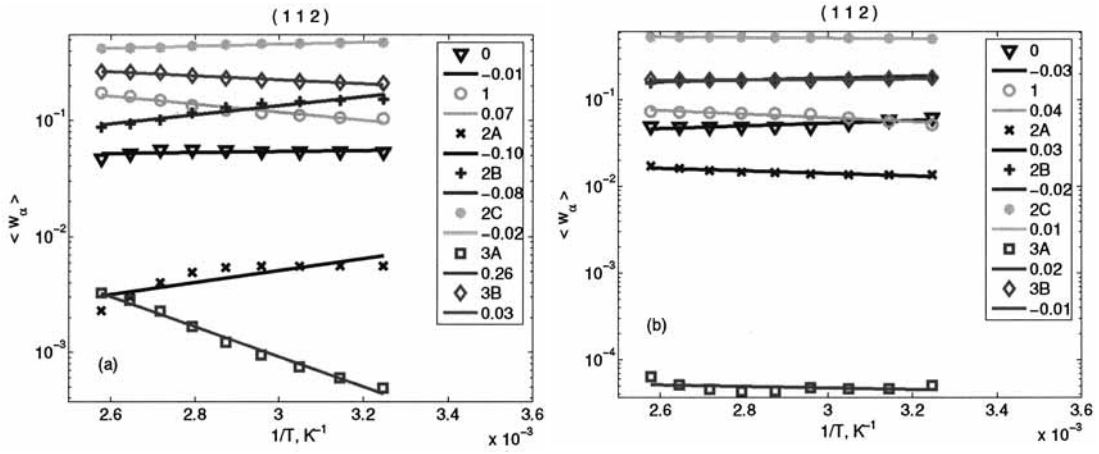

Fig. 6. (Approximate) relative contributions of each surface site ($\alpha = 1, 2A, 2B,...$) to the macroscopic activation energy using the parameters of (a) case B and (b) case A for a representative orientation (211). Activations energies (in eV) are calculated as the slopes of the linear fits.

Acknowledgments

This research has been supported by the Academy of Finland through its Center of Excellence Programme (2000–2005) and by the Finnish Academy of Science and Letters, Vilho, Yrjö, and Kalle Väisälä Foundation. M. A. G. is thankful to A. Paalanen for providing the results shown in Fig. 3.

References

1 H. Seidel, L. Csepregui, A. Heuberger and H. Baumgärtel: J. Electrochem. Soc. **137** (1990) 3612.
2 M. Shikida, K. Sato, K. Tokoro and D. Uchikawa: Sensors and Actuators **80** (2000) 179.
3 M. A. Gosálvez and R. M. Nieminen: Phys. Rev. E **68** (2003) 031604.
4 M. A. Gosálvez, A. S. Foster and R. M. Nieminen: Europhysics Letters **60** (2002) 467.
5 M. A. Gosálvez, A. S. Foster and R. M. Nieminen, Appl. Surf. Sci. **202** (2002) 160.
6 N. Metropolis, A. W. Rosenbluth, M. N. Rosenbluth, A. H. Teller and E. Teller: J. Chem. Phys. **21** (1953) 1087.
7 J. Kasparian, M. Elwenspoek and P. Allongue: Surf. Sci. **388** (1997) 50.
8 M. A. Gosálvez and R. M. Nieminen: New J. Phys. **5** (2003) 100.